



Design and Analysis of 80cc, 4-Stroke Spark Ignition Engine Connecting Rod

R.S. Ebhojiaye^a and C.I. Eboigbe^b

^{a*,b} Department of Production Engineering, University of Benin, Benin City, Edo State, Nigeria

^{a*}aphael.ebhojiaye@uniben.edu, ^bChristopher.eboigbe@uniben.edu

Article Info

Keywords:

Von Mises Stress, Connecting Rod, Aluminium Alloy, Yield Stress, simulation.

Received 07 May 2022

Revised 18 May 2022

Accepted 29 May 2022

Available online 14 June 2022



<https://doi.org/10.37933/nipes.e/4.2.2022.28>

<https://nipesjournals.org.ng>

© 2022 NIPES Pub. All rights reserved

Abstract

In this study, the connecting rod was designed and simulated to determine its performance under real condition of service. The designed parameters of the connecting rod were modeled into 3-D geometry using SOLIDWORKS software. The 3-D model was imported into the static structure environment of the ANSYS software. Finite element analysis was conducted to ascertain the variation of stress magnitude at critical locations of the connecting rod. The load boundary condition in static simulation model was determined by the ideal gas equation. The engine specification chart was used to get the other simulation inputs that were used. Maximum deformation of 0.062428mm was recorded at the small end of the connecting rod because the material thickness was unable to support the applied force at the end of the rod. The simulation results showed that von Mises stress present in the aluminum alloy (2024-T361) rod was less than its yield strength indicating that there can be material saving in the lowest stressed region.

1.0 Introduction

The connecting rod shown in Figure 1 links the piston pin to the connecting rod journal or crankpin on the crankshaft. It joins the piston to the crankshaft and is responsible for conveying power from the piston to the crankshaft and sending it to the transmission [1]. It consists of a pin-end, a shank section, and a crank-end. Pin-end and crank-end pinholes at the upper and lower ends are carefully machined to permit accurate fitting of bearings. In internal combustion engines, the connecting rods are usually made of steel but other materials like aluminum, cast iron and titanium are also used in the production of connecting rods [2]. In the design of an engine, the connecting rod is treated as a critical component. Therefore, effort is made to minimize residual stress by shot peening to reduce compressive stresses, balancing the weight to all connecting rod assemblies, grinding the edges of the rod to a smooth radius and magna-fluxing to reveal very minute cracks which could cause the rod to fail under stress [3,4]. This component is the most common cause of catastrophic engine failure. It is under an enormous amount of load pressure and is often the recipient of special care to ensure that it does not fail prematurely. In most high-performance applications, the connecting rod is balanced to prevent unwanted harmonics from creating excessive wear. Mohankumar and Rakesh [5] described the connecting rod as the component that transfers power to the crank which is turned to rotational power. A connecting rod can be of two types H-beam or I-beam or a combination of both. The high cost of manufacturing aluminium alloy and steel which are the most used materials for the design of piston and connecting rod respectively makes one conscious of wastages generated during the manufacturing of this products. Also, there is a recent trend in the reduction of connecting rod weight to reduce inertia.

Studies were carried out by [6,7] on the design and analysis of connecting rod. The research showed that high stress near web and flange of connecting rod were as a result of poor material selection and design. Considering the need to design and innovate cheap and effective internal engine components, this study has contributed to solving this problem.



Figure 1: The Connecting Rod [8]

2.0.Method

The following parameters were considered for the connecting rod design. They included dimension of cross-section, dimension of the crankpin at the big end and the piston pin at the small end, size of bolt for securing the big end cap, and thickness of the big end cap.

2.1.Material Selection

The connecting rod design was done with respect to aluminum alloy material. The mechanical properties of the aluminium alloy used for the research analysis was that of aluminum 2024-T361. The material selection was based on the design done, its availability and low cost. The chemical composition, mechanical properties, engine specifications and Cylinder parameters of the aluminium alloy material used for the design are shown in Tables 1, 2, 3 and 4 respectively [9]. According to [10], the connecting rod is exposed to a complex state of loading. It experiences huge cyclic loads of about 108 to 109 cycles, which ranged from high compressive loads to high tensile loads due to inertia. The durability of the connecting rod component is of critical importance.

Table 1: Chemical Composition of the 2024-T361 Aluminium Alloy Material

Element	Content (%)
Aluminum (Al)	90.8 to 94.7
Copper (Cu)	3.8 to 4.9
Magnesium (Mg)	1.2 to 1.8
Manganese (Mn)	0.3 to 0.9
Iron (Fe)	Max 0.5
Silicon (Si)	Max 0.5
Zinc (Zn)	Max 0.25
Titanium (Ti)	Max 0.15

Table 2: Physical and Mechanical Properties of the 2024-T361 Aluminium Alloy Material

Properties	Values
Elastic Modulus	72.4 GPa
Poisson’s Ratio	0.33
Shear Modulus	28 GPa

Density	2780 kg/m ³
Tensile Strength	495 Mpa
Yield Strength	395 Mpa
Thermal Conductivity	120 W/m-K

Table 3: Engine specification (80cc, 4 strokes air-cooled petrol engine)

PARAMETERS	VALUES
Engine Type	Four strokes, Petrol Engine
Induction	Air cooled Type
Number of Cylinders	Single Cylinder
Bore	45.1mm
Stroke	50.10mm
Length of Cylinder	57.67mm
Displacement Volume	80.035mm ³
Number of Revolutions/Cycle	2

Table 4: Standard values of Cylinder parameters

Mechanical efficiency of the engine	0.8
Density of petrol	737.22kg/m ³
Molecular weight of petrol	114.2285 g/mole
Gas constant	8.314 J/mole-k

2.2 Design

A connecting rod is a machine member which is subjected to alternating direct compressive and tensile force. Since the compressive forces are much higher than the tensile forces, the cross-section of the connecting rod was design as a strut with respect to the rod length. The Rankine Gordon formula [11] was used to determine the connecting rod axial load (W) in both the x-axis and the y-axis.

About the x-axis, the axial load (W_x) is

$$W_x = \frac{f_{cu} \times A}{1 + a \left(\frac{L}{k_x}\right)^2} \quad (1)$$

where, A = cross-sectional area of the connecting rod, m²

k_x = radius of gyration of the section about x-axis, m

l = length of the connecting rod, m

f_{cu} = ultimate crushing stress, N/m²

a = constant.

According to [12], if both ends are hinged, $L = l$.

$$\therefore W_x = \frac{f_{cu} \times A}{1 + a \left(\frac{l}{k_x}\right)^2} \quad (2)$$

About the y-axis, the axial load (W_y) is

$$W_y = \frac{f_{cu} \times A}{1 + a \left(\frac{L}{k_y}\right)^2} \quad (3)$$

Also, according to [13], for both ends fixed, $L = l/2$.

$$\therefore W_y = \frac{f_{cu} \times A}{1 + a \left(\frac{l}{2k_y}\right)^2} \quad (4)$$

According to [14], for the connecting rod to be equally strong in buckling about both the x and y axes, the buckling loads must be equal.

$$\therefore \frac{f_{cu} \times A}{1+a\left(\frac{l}{k_x}\right)^2} = \frac{f_{cu} \times A}{1+a\left(\frac{l}{2k_y}\right)^2}$$

$$\therefore \left(\frac{l}{k_x}\right)^2 = \left(\frac{l}{2k_y}\right)^2$$

$$k_x^2 = 4k_y^2 \tag{5}$$

$$\therefore I_x = 4I_y \tag{6}$$

where, I_x = moment of inertia of the section about x-axis,
 I_y = moment of inertia of the section about y-axis.

From Eq. (6) it can be implied that the connecting rod is four times stronger in buckling about the y-axis than about the x-axis. The most suitable section for the connecting rod is I-section [15] as shown in Figure 2.

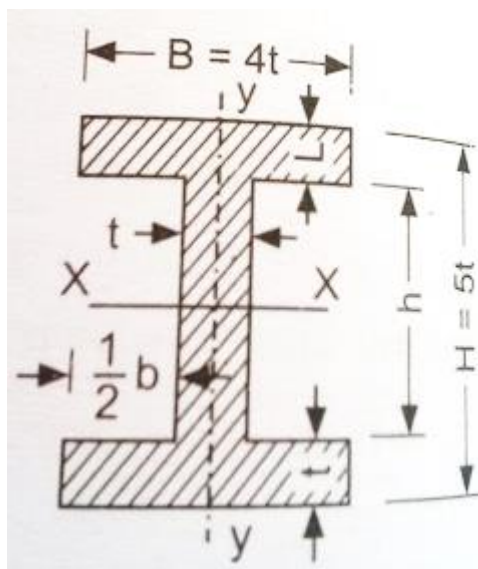


Figure 2: I-Section of the connecting rod

From Figure 2, the flange and web thickness of the section = t

Depth of section, $h = 5t$

Width of section, $b = 4t$

$$\therefore \text{Area of section, } A = 11t$$

Moment of inertia about x-axis:

$$I_x = \frac{1}{12} [4t (5t)^3 - 3t(3t)^3] \tag{7}$$

Also, moment of inertia about y-axis:

$$I_y = \frac{2}{12} [t(4t)^3 + \frac{1}{12} (3t)t^3] \tag{8}$$

$$\therefore \frac{I_x}{I_y} = \frac{\frac{419}{12}}{\frac{131}{12}} = 3.2$$

According to [16], the I_x/I_y ratio is usually taken as between 3 and 3.5. Therefore, the value of 3.2 obtained showed that the proportions of the I-section are suitable.

2.2.1 Determination of the cross-section area, A

According to [17], the cross-section area and the moment of inertia of the cylinder rod can be determined using Equations 8,9 and 10.

$$A = 2(4t \times t) + 3t \times t \tag{8}$$

$$= 11t^2$$

Where;

t = Thickness of flange

Moment of inertia about x-axis

$$I_{xx} = \frac{1}{12} [4t\{5t\}^3 - 3t\{3t\}^3]$$

$$I_{xx} = \frac{419t^4}{12} \tag{9}$$

And moment of inertia about y-axis

$$\frac{2}{12} \times t \times \{4t\}^3 + \frac{1}{12} \{3t\}^3$$

$$I_{yy} = \frac{131t^4}{12} \tag{10}$$

$$\frac{l_{xx}}{l_{yy}} = \frac{419 \times 12}{12 \times 131} = 3.2$$

Since the value of $\frac{l_{xx}}{l_{yy}}$ lies between 3 and 3.5 m, therefore I-section chosen is quite satisfactory.

2.2.2 Determination of the Maximum Gas Pressure

According to [18], the design calculations for the cylinder are considered under the maximum pressure condition as follows:

Density of Petrol:

$$\begin{aligned} C_8H_{18} &= 737.22 \text{ kg/m}^3 \text{ at } 60^\circ\text{F} \\ &= 0.00073722 \text{ kg/cm}^3 \\ &= 0.00000073722 \text{ kg/mm}^3 \end{aligned}$$

$$\begin{aligned} T &= 60^\circ\text{F} \\ &= 288.855\text{K} \\ &= 15.55^\circ\text{C} \end{aligned}$$

$$\begin{aligned} \text{Mass} &= \text{Density} \times \text{Volume} \\ m &= 0.00000073722 \times 80035 \end{aligned}$$

$$m = 0.059 \text{ kg}$$

Molecular weight for petrol 114.2285 g/mole

$$PV = MRT \tag{11}$$

Where, M = mass/molecular weight

R = Gas constant

T = Temperature in kelvin

$$P = \frac{0.059 \times 8.31430 \times 288.855}{0.1142285 \times 8.0035 \times 10^{-5}}$$

$$P_{\max} = 9.389 \text{ MPa}$$

2.2.3 Calculation for Buckling Load (W_B)

The analyses of the buckling load and other vital connecting rod parameters by [19] are shown in equations 12 to 19.

Buckling Load, W_B is given as:

$$W_B = \frac{\pi D^2}{4} \times p_{\max} \times F.O.S \tag{12}$$

Where

F.O.S = Factor of safety

The material is aluminum alloy whose tensile strength is 495MPa and F.O.S is 5.5

$$W_B = \frac{\pi \times 45.1^2}{4} \times 9.389 \times 5.5$$

$$W_B = 82500\text{N}$$

$$K_{xx} = \left(\frac{I_{xx}}{A}\right)^{\frac{1}{2}} \quad (13)$$

$$K_{xx} = 1.78t \quad (14)$$

2.2.4 Calculation for Width of the flange

The width of section given as

$$B = 4t$$

$$B = 4 \times 7.33$$

$$B = 29.32\text{mm}$$

2.2.5 Calculation for Height of the flange

The height of section is given as

$$H = 5t$$

$$H = 5 \times 7.33$$

$$H = 36.65\text{mm}$$

2.2.6 Calculation for Area of the connecting rod

$$\text{Area, } A = 11t^2$$

$$= 11 \times 7.33 \times 7.33$$

$$= 591.01\text{mm}^2$$

2.2.7 Calculation for Height of the big crank end

Height at the big end (crank end), H_2 is taken from

$$H_2 = 1.1H \text{ to } 1.25H \quad (17)$$

$$H_2 = 1.1 \times 36.65$$

$$H_2 = 40.32\text{mm}$$

2.2.8 Calculation for Height of the small crank end

Height at the small end (piston end), H_1 is taking from

$$H_1 = 0.9H \text{ to } 0.75H \quad (18)$$

$$H_1 = 0.9 \times 36.65$$

$$H_1 = 32.99\text{mm}$$

$$\text{Stroke length (l)} = 50.1 \text{ mm}$$

$$\text{Diameter of piston (D)} = 45.1\text{mm}$$

$$P = 9.389\text{N/mm}^2$$

$$\text{Radius of crank (r)} = \frac{\text{stroke of length}}{2} \quad (19)$$

$$= \frac{50.1}{2}$$

$$= 25.05\text{mm}$$

2.2.9 Calculation for the Maximum Angular Speed

The maximum angular speed and other parameters related to the design of the connected rod in equations 20 to 26 were obtained from [20].

Maximum angular speed is given as

$$W_{\max} = \frac{2 \times \pi \times N_{\max}}{60} \quad (20)$$

$$W_{\max} = \text{speed per revolution}$$

$$W_{\max} = \frac{2 \times \pi \times 8500}{60}$$

$$W_{\max} = 890\text{rad/s}$$

2.2.10 Calculation for the maximum inertia force

The maximum Inertia force of reciprocating parts, F_{im} is given as

$$F_{im} = m \times r \times W_{max}^2 \times r \left(1 + \frac{1}{n}\right) \quad (21)$$

$$F_{im} = 0.059 \times 890^2 \times 0.02505 \times \left(1 + \frac{1}{4}\right)$$

$$F_{im} = 1463.36\text{N}$$

2.2.11 Calculation for the Inner diameter of the small end

The Inner diameter of the small end, d_1 is given as

$$d_1 = \frac{F_{im}}{Pb_1 \times l_1} \quad (22)$$

Where,

Design bearing pressure for small end $pb_1 = 12.5$ to 15.4N/mm^2

Length of the piston pin, $l_1 = (1.5$ to $2)$

$$d_1 = \frac{1463.36}{12.5 \times 1.5}$$

$$= 32.34\text{mm}$$

2.2.12 Calculation for the outer diameter of the small end

Outer diameter of the small end, $d_o = d_1 + 2t_b + 2t_m$

$$= 32.34 + [2 \times 2] + [2 \times 5]$$

$$= 46.34\text{mm}$$

Where,

Thickness of the bush (t_b) = 2 to 5 mm

Marginal thickness (t_m) = 5 to 15 mm

2.2.13 Calculation for the inner diameter of the small end

$$\text{Inner diameter of the big end } d_i = \frac{f_g}{Pb_2 \times l_2} \quad (23)$$

$$= \frac{19609.4}{10.8 \times 1 \times 46.34}$$

$$= 42.61\text{mm}$$

Where,

Design bearing pressure for big end $pb_2 = 10.8$ to 12.6N/mm^2

Length of the crank pin $l_2 = (1.0$ to $1.25)$

2.2.14 Calculation for the root diameter of the bolt, d_r

$$\text{Root diameter of the bolt, } d_r = \frac{2f_{im}}{\sqrt{\pi s_t}} \quad (24)$$

$$= \frac{2 \times 6277.167}{\sqrt{\pi \times 56.667}} = 4\text{mm}$$

2.2.15 Calculation for outer diameter of the big end

$$\text{Outer diameter of the big end, } D_e = d_2 + 2t_b + 2d_b + 2t_m \quad (25)$$

$$= 42.65 + (2 \times 2) + (2 \times 4) + (2 \times 5)$$

$$= 64.61\text{mm}$$

Where,

Thickness of the bush, $t_b = 2$ to 5 mm

Marginal thickness, $t_m = 5$ to 15 mm

2.2.16 Calculation for the nominal diameter of the bolt

$$\text{Nominal diameter of bolt, } d_b = 1.2 \times d_r \quad (26)$$

$$= 1.2 \times 4$$

$$= 4.8\text{mm}$$

Figures 3 and 4 are the modelled and orthographic projections of the connecting rod.

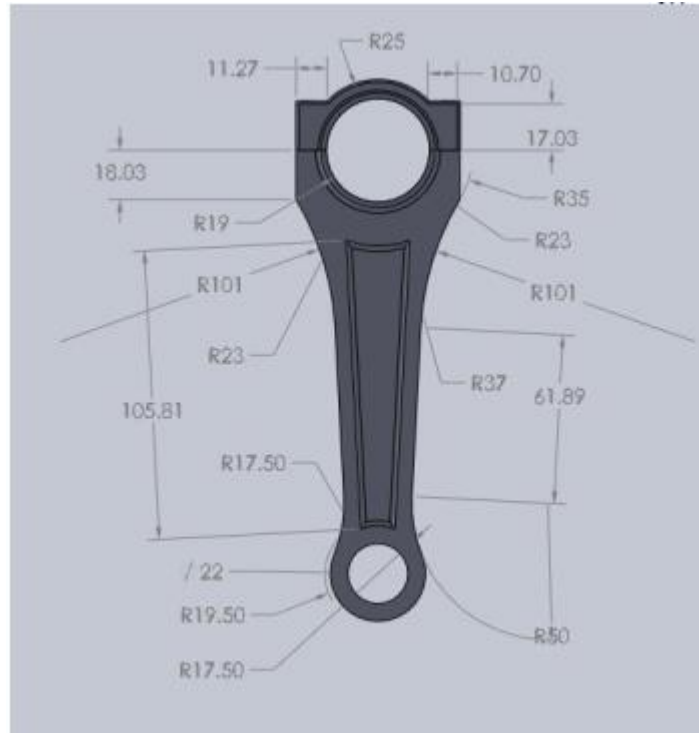


Figure 3: Modelled Connecting rod dimensioned in mm

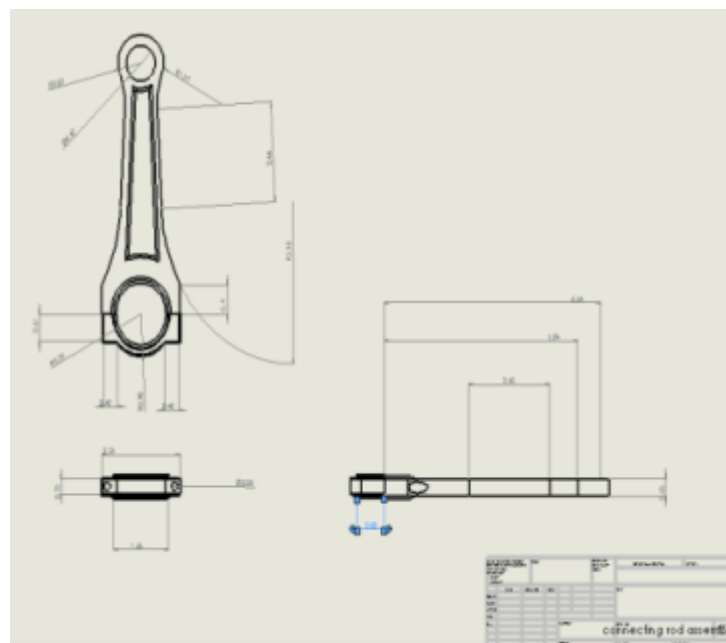


Figure 4: Orthographic projection of connecting rod

3.0 Results and Discussion

The connecting rod was simulated to see how it will behave under well specified conditions. The mesh type used was a solid mesh and a curvature base mesh. The element size was taken as 2.0mm, then total number of elements were 12567 and the total nodes were 23193.

3.1 Static Structural

The simulation done in ANSYS took into account the buckling load applied to the connecting rod.

This will give an idea of what will be the tensions in the whole connecting rod. Figure 5 shows the Von Mises stress on the rod.

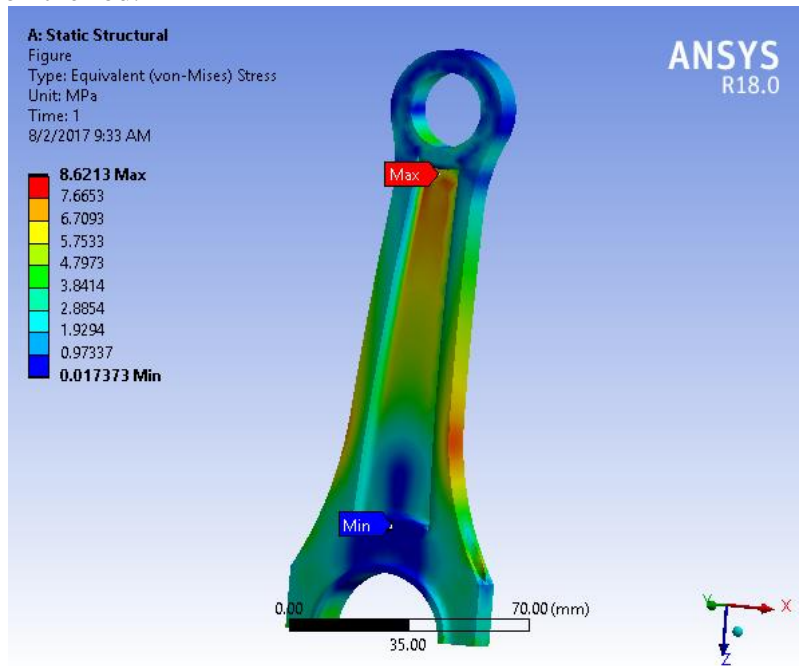


Figure 5: Von Mises stress

In Figure 5, it can be seen that the parts that suffer the most is the smaller end of the connecting rod where the piston is joined. The pressure on the connecting rod is 9.38MPa. As expected, the smaller end of the connecting rod suffers because it 'bears the pressure from the piston. The fillet radius of the small end region on the connecting rod should be increased in order to decrease the value of the stress obtained. Figure 6 shows the total deformation in the rod.

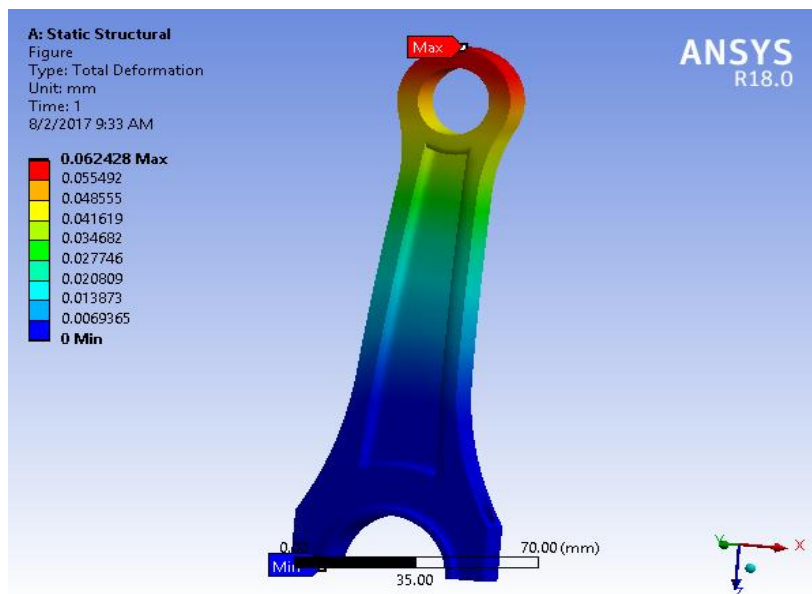


Figure 6: Total deformation

It can be seen that the biggest deformation takes place in the extreme of the smaller end of the connecting rod. Figure 7 shows the normal Stress on the connecting rod.

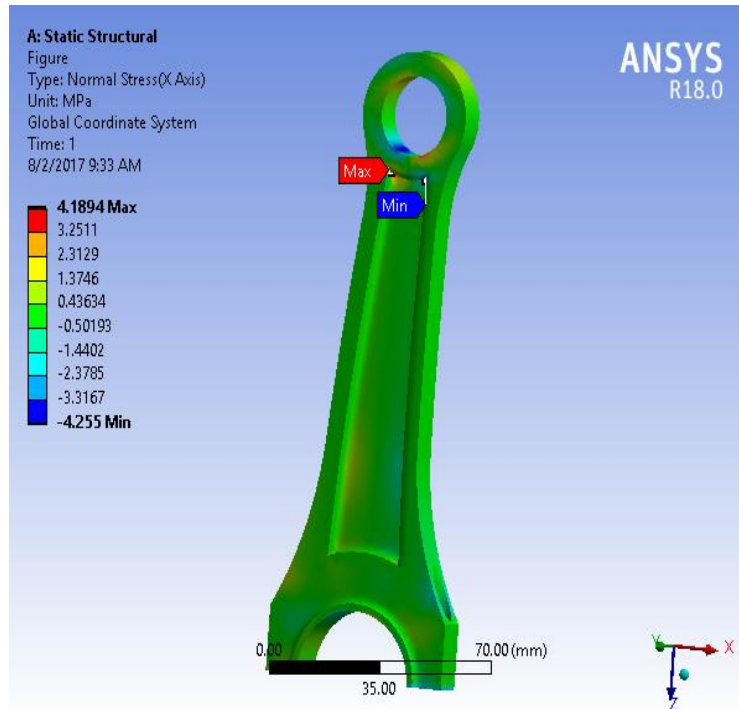


Figure 7: Normal stress

The values obtained for the stress distribution on the connecting rod are acceptable because the stress is minimal.

Table 3 displays the maximum and minimum values of the stresses and total deformation observed in the connecting rod after the simulation.

The results show that the max von Mises stress is smaller than the allowable design stress for the material aluminum alloy 2024-T361 (Max von Mises stress < Allowable design stress). A deformation of 0.062428mm was recorded at the small end of the connecting rod and this is due to its thickness and the corresponding force from the piston.

Table 3: Stresses for Connecting rod

Serial number	Type	Min	Max
1.	Equivalent stress	0.017373 Mpa	8.6213 Mpa
2.	Total deformation	0	0.062428 mm
3.	Normal stress	-4.255Mpa	4.1894Mpa

4.0. Conclusion

The connecting rod is a vital part of internal combustion engine. The weight can be reduced by using aluminium alloy (2024-T361) material. The result from the simulation shows that deformation is peak at the extreme end of the connecting rod. Therefore, increasing the thickness of the small end of the rod will minimize the deformation. The values obtained for the stress distribution was acceptable because the stress was minimal.

References

- [1] N.P.Doshi, N.K.Ingole (2013). Analysis of Connecting Rod Using Analytical and Finite Element Method. International Journal of Modern Engineering Research (IJMER). Vol.3, Issue.1, pp-65-68.
- [2] S. Sathishkumar, B.Dinesh, K.Praveen, J.Surendar (2018). Material Optimization and Structural Analysis of Internal Combustion Engine Connecting Rod and Shaft. International Journal of Innovative Research in Technology.Vol.4, pp.1234-1242.

- [3] O.Jamkhedkar, K. Marathe, M.Pawar, P. Khanvikar, S.Gaonkar (2018). Enhancement in Performance of Connecting rod using Surface process. International Journal of Engineering Science Invention. Vol.7, pp.65-73.
- [4] S.R. Thilagavathy, C.Manjula, M. Inbavalli, A.K. Sathyakala (2019). Design and Optimization of two wheeler Connecting rod using an alloy. International Journal of Applied Engineering Research. Vol. 14, pp. 200-220.
- [5] D.Mohankumar and L. Rakesh (2017). Design and Analysis Of A Connecting Rod. International Journal of Pure and Applied Mathematics, Volume 116, pp. 105-109.
- [6] S.Khare, O.P.Singh, K.b.dora and C. Sasun (2012).Spalling investigation of connecting rod. Science Direct, Engineering failure analysis 19: pp.77-86.
- [7] L.K. Vegil, V.G.Vegi (2013). Design and analysis of connecting rod using forged steel. International Journal of Scientific and Engineering research. Vol.4, pp.2081- 2090.
- [8] A.R.Varma, R.Ramachandra (2017). Design and analysis of 150CC IC Engine Connecting Rod. International Journal of Scientific Research in Science and Technology. Vol.3, pp.891-904.
- [9] S.M. Beden, S.Abdullah, A.K.ariffin, N.A.Al-Asady (2010). Fatigue crack growth simulation of aluminium alloy under spectrum loadings.Materials and Design. Vol.31, pp.3449 – 3456.
- [10] V.Ganeshram, M.Achudhan (2013). Design and analysis of piston cooling nozzle in automobiles. Indian Journal of Science and Technology.Vol.6, pp-4808-4813.
- [11] P. C. Sharma, D. K. Aggarwal (2012). A Textbook of Machine Design (in S.I. Units).Edition, 12, Publisher, S.K. Kataria.
- [12] M.k.Pal and T.D.Wasim (2014).Analysis (Stress strain and Displacement) and optimization of connecting rod using AIFA SiC Composites. International Journal of Civil and structural Engineering. Vol.1, pp.22-26.
- [13] B.Kuldeep, L.R.Arum, M.Faheem (2013).Analysis and optimization of connecting rod using ALFA SiC composites. International Journal of Innovative Research in Science, Engineering and Technology.Vol.2, pp 2480 – 2487.
- [14] Sushant, V.Gambhir (2014). Design and Comparative Performance Analysis of Two Wheeler Connecting Rod Using Two Different Materials Namely Carbon70 Steel and Aluminum 7068 by Finite Element Analysis . International Journal of Research in Aeronautical And Mechanical Engineering. Vol.2, pp.63 -78.
- [15] V.K Verma, S.Kumar, A. Gupta (2016). FE Modeling of I-SECTION Connecting Rod. International Journal of Advanced Research in Science, Engineering and Technology.Vol.3, pp.2740 – 2748.
- [16] G. Naga- Malleshwara (2013). Design Optimization and Analysis of a Connecting Rod using ANSYS. International Journal of Science and Research. Vol.2, pp.225-229
- [17] O.Parkash, V.Gupta, V. Mittal (2013). Optimizing the Design of Connecting Rod under Static and Fatigue Loading. International Journal of Research in Management, Science & Technology, Vol. 1, pp. 39-43.

- [18] K.Sivaramkrishnan, G.Jithendra, V. Kumar (2019). Design and Analysis of four stroke engine piston. International Journal of Engineering Science and Computing.Vol.9, pp. 19743- 19746.
- [19] H.D.Nitturkar, S.M. Kalshetti, A.R..Nadaf (2020). Design and Analysis of Connecting rod using different materials. International research journal of Engineering and Technology. Vol.7, pp.1011-1017.
- [20] M. Hariharan, V. Kalaigowtham, S. Aravind, P. Parandaman, A.Selvaraj (2020). Design and Analysis of manganese alloy steel connectin rod. International Journal of Engineering Applied Sciences and Technology. Vol.4, pp.562-569.